New approach to estimate macro and micronutrients in potato plants based on foliar spectral reflectance

Reem Abukmeil[1], Ahmad Al-Mallahi[1, *], Felipe Campelo[2]

[1] Department of Engineering, Faculty of Agriculture, Dalhousie University, Nova Scotia, Canada

[2] Department of Computer Science, Aston University, Birmingham, United Kingdom

[*]Corresponding author: ahmad.almallahi@dal.ca

Abstract: Tissue testing used to assess the chemical contents in potato plants is considered laborious, time-consuming, destructive, and expensive. Ground-based sensors have been assessed to provide efficient information on nitrogen using leaf canopy reflectance. In potatoes, however, the main organ required for tissue testing is the petiole to estimate the elements of all nutrients. This research aims to assess whether there is a correlation between the chemical contents of potato petioles and leaf spectrum, and to examine whether the spectrum of dried or fresh leaves have higher correlation values. Petiole chemical contents of all elements were tested as a reference point. Leaves were split equally into dried and fresh groups for spectral analysis (400-2500 nm). Lasso Regression models were built to estimate concentrations in comparison to actual values. The performances of the model were tested using the Ratio of (standard error of) Prediction to (standard) Deviation (RPD). All elements showed reasonable to excellent RPD values except for sodium. All elements showed higher correlation in the dried testing mode except for nitrogen and potassium. The models showed that the most significant wavebands were in the visible and very near infrared range (400 - 1100 nm) for all macronutrients except magnesium and sulfur, while all micronutrients had the most significant wavebands in full range (400 - 2500 nm) with a common significant waveband at 1932 nm. The results show high potentials of a new approach to estimate potato plant elements based on foliar spectral reflectance.

Key words: Spectroscopy, petiole, macronutrients, micronutrients, multiple linear regression

Nomenclature

N	Nitrogen	y	Chemical results of petioles
P	Phosphorus	x_i	Spectral results of the leaves of the *i*-th waveband
K	Potassium	B_i	Regression coefficient of the *i*-th waveband
Ca	Calcium	$\beta_\circ$	Intercept
Mg	Magnesium	Z	Vector of spectrum inputs
S	Sulfur	r^2	Coefficient of determination
Mn	Manganese	r	Pearson's correlation
Zn	Zinc	SD	Standard deviation
Fe	Iron	SEP	Standard Error of Prediction
Na	Sodium	RPD	Ratio of (standard error of) Prediction to (standard) Deviation
Cu	Copper	C	Number of datapoints
Al	Aluminum	A_n	Actual concentrations at *n*-th datapoint from 1 to C
B	Boron	E_n	Estimated concentrations at *n*-th datapoint from 1 to C
Vis	Visible range	n	Index of datapoint 1, …, C-1, C
VNIR	Very near infrared	λ	Complexity parameter (Lambda)
SWIR	Short wave infrared		

1. Introduction

In Canada, potatoes (*Solanum tuberosum L*) are the largest vegetable crop accounting for 27.2% and 14.7% of all vegetable and horticultural receipts, respectively (Agriculture and Agri Food Canada, 2020). Since the early 1990s, Canadian potato production has expanded to meet international demand for frozen potato products (International year of the potato, 2008). Potato growers have then integrated management schemes to increase the production efficiency (Bohl and Johnson, 2010). One of these management schemes is to evaluate the level of inputs of fertilizers to produce quality potato tubers (Torabian et al., 2021).

The nutritional composition of potato tubers is responded by the availability of both macro and micronutrients for plant uptake (Naumann et al., 2020). Macronutrients such as nitrogen (N), phosphorus (P), potassium (K), calcium (Ca), magnesium (Mg), and sulfur (S) are needed in large quantities with respect to their physiological functions in plant metabolism and for tuber yield formation (Koch et al., 2020). Also, the micronutrients such as manganese (Mn), zinc (Zn), iron

(Fe), sodium (Na), copper (Cu), aluminum (Al), and boron (B), whose inclusion in the fertilizer schedule is very essential to sustain production and quality, are needed in small quantities.

Commonly, nutrients are applied either by soil or foliar treatments. However, as soil application is sometimes incapable to supply the nutrients in adequate quantity (Moinuddin et al., 2017), foliar application can be more efficient in the supply of nutrients (AL-Jobori and AL-Hadithy, 2014). Therefore, proper identification of nutritional status of crop species is important for foliar application to correct the diagnosis of nutrient deficiencies.

Current methods such as visual diagnosis, plant tissue tests, soil tests, and cropping history are frequently used to assess nutrient deficiencies before taking the decision of application (Fageria et al., 2009). Among these methods, tissue tests were declared to be the most accurate (Motsara and Roy, 2008). However, the credibility of tissue testing immensely depends on the time gap between sample collection and testing. A study stated that tissue testing can be a credible tool for deficiency diagnosis when the tissue samples for vegetable crops are collected from the field, shipped to the laboratory, and analyzed in the lab in the next day, otherwise remedial actions would be disrupted (Hochmuth et al., 2018). Therefore, a rapid, efficient, and cost-effective techniques for routine analysis to identify nutritional status is needed (Liao et al., 2012).

Non-destructive techniques have been used to provide efficient information on the plant functional traits including nutrient contents using leaf/ canopy reflectance (Herrmann and Berger, 2021). The concept of such techniques is based on the reflectance of visible light and near infrared which have proportional relationships with the chlorophyll content (Povh, and dos Anjos, 2014). Previous research found that significant spectral bands in forestry and crop applications exist at the visible and very near infrared (Vis-VNIR, 400 - 1100 nm) and in short wave infrared (SWIR, 1000 - 3000 nm) (Saari et al., 2011).

Ground-based sensors, based on vegetation indices using specific wavelengths, are delivered to markets to estimate plant properties (Gabriel et al., 2017). Also, remote sensors are widely used to detect stressed plants by obtaining the electromagnetic wave reflectance information from canopy as the leaf area index (LAI) (Xue and Su, 2017). However, both sensors have drawbacks related to canopy reflectance including atmospheric and soil interference (Muñoz-Huerta et al., 2013). Several studies then analyzed the reflectance at the leaf level to eliminate the noise coming from atmospheric and soil interference such as Mahajan et al. (2021), Peng et al. (2020) and Liao et al. (2012). These studies relate the specific waveband found to the chemical analysis of the leaves as a reference point. Several studies have been done to detect N deficiencies using spectral results in different testing modes. Testing modes of leaves are differentiated into intact analysis directly in the field (fresh, intact leaves), fresh leaves removed from the plants for laboratory scanning (fresh removed leaves), and dried and ground leaf samples (dried ground leaves) (Prananto et al., 2020). A study done by Zerner and Parker (2019) estimated N using NIRS (350 nm - 1100 nm) on fresh/ intact wheat leaf in comparison to dried ground wheat leaves. In other studies, poor calibration models were found based on the analysis of fresh leaves such as the ones built by Rotbart et al. (2013) for olive leaf N, and Menesatti et al. (2010) for orange leaf P. Rotbart et al. (2013) refers the reason that leaf dehydration improves the model performance significantly by to a better calibration for N estimation using dried ground olive leaves, over fresh/ intact leaves.

Predicting foliar nutrients other than N is still limited and their deficiency diagnosis still follows destructive methods. For fingered citron, a good calibration model was obtained for P, K, F, and Mn in dried leaves, whereas the prediction of Cu and Zn were poorly reliable (Liao et al., 2012). Another research studied the possibility to estimate leaf NPK contents in temperate degraded vegetation using the wavelength range of 325 to 1075 nm (Peng et al., 2020). Their research demonstrated that the sensitive wavebands for P were in the green and NIR regions, and the sensitive bands for K were in the green, red and NIR regions.

However, petioles are the main organ for tissue testing in potato plants. Nevertheless, spectrum over a petiole is impractical due to its thin shape that will not fill the ground of a handheld spectrophotometer or a cup for lab spectrophotometer. Moreover, collecting the petioles is destructive because there is a need to collect 40 to 50 petioles per sample for adequate lab analysis (Rowe, 1993). Therefore, few research has been ongoing to find the correlation between leaf spectrum and petiole chemical testing rather than leaf chemical testing. A study concluded a significant relationship between leaf reflectance and petiole nitrate-N for Ranger Russet and Russet Burbank early in the growing season with coefficient of determination values up to 0.65 (Davenport et al., 2005). Another study showed a strong correlation between petiole nitrate concentration of Russet Burbank and Shepody potato cultivars and leaf protein content for Russet Burbank, with correlation coefficients ranging between 0.48 and 0.89, and a strong correlation between petiole nitrate concentration and chlorophyll content with correlation coefficients not less than 0.63 (Botha et al., 2006). One more study assessed the relationships between leaf spectral reflectance at 400 - 900 nm and N levels in potato petioles and leaves for the purpose to assess the potential of a satellite to perform spatial analysis of nitrogen levels in potatoes (Cohen et al., 2010). Another work used imaging spectroscopy to predict foliar nitrogen and petiole nitrate at different wavelength regions of different potato cultivars and planting seasons (Liu et al., 2021)

There are no studies that compared the results of NIRS between leaves with petiole chemical testing for nutrients other than N. In addition, spectral analysis using the full spectrum (400 - 2500 nm) have not been widely tested for utility in predicting potato nutrient status. Therefore, the overall purpose of this research work is to investigate whether there is a correlation between the chemical testing of potato petioles and leaf spectral data, and to examine which testing mode of dried or fresh leaves has higher correlation in a lab-based level. Our analysis includes all macro and micronutrients investigated by farmers in Canada. The results of this research will be used into further analyses to build validated robust models.

2. Materials and Methods

2.1. Sample preparation

The experiment of this research work followed the current protocol of sample collection, preparation, and chemical testing by potato growers in NB, Canada. A total of 40 datapoints of Russet Burbank, the major potato variety in NB, Canada, were taken from sub plots at two potato farms in the Lakeville of New Brunswick in season, and hereafter is called farm data. Sampling was performed from late June (40 - 45 days after planting), to late September 2020. This sampling covers a period when measurement of crop nutrient status could give the best results (Zebarth et al., 2007). Other 20 datapoints were taken at sub plots from an indoor cultivation area from September to December 2020 at the Department of Engineering in the Agriculture Campus of Dalhousie University in Truro, Nova Scotia, and hereafter is called indoor data. The indoor cultivation was implemented to increase datapoints to the dataset.

The typical grower practice is to band-apply all fertilizer at the planting stage in Atlantic Canada (Zebarth et al., 2004). Thus, indoor cultivation area gives us the opportunity to apply different fertilization schemes. We followed an over application for NPK in one group (20-20-20 NPK application) and a cut in P content for the second group (22-0-22 NPK weekly) from the fourth week until the end of the season.

At each location (the two farms in Lakeville and the indoor area at Dalhousie University), sampling took place every other week as per the protocol in Atlantic Canada (Zebarth et al., 2007). Figure 1 shows the steps taken for sampling and analysis. Both petiole and leaf samples from the farm were collected from the fourth leaf from the apex of the shoot on healthy plants (Rowe, 1993). Each datapoint contained 40 petioles and 40 leaves for lab chemical testing. This quantity of petioles is also required by the DairyLand Lab inc. (Arcadia, Wisconsin, USA), at where the analysis took place, to give a dry weight of 3 gram necessary for chemical testing. The leaves were split equally into two groups, labelled as fresh and dried, with 20 in each. The leaves and petioles were immediately vacuum packed into sampling bags after peeling them off and refrigerated before shipment. At each location, sampling was random within the same sub plot over the season. The samples were packed with ice bag and the time lag until reception by lab was two days. The leaves were analyzed for their spectral reflectance using NIRS Analyzer (DS2500, Metrohm USA Inc.) (Table 1). The leaves and petioles were dried at 55 - 60 degree Celsius (°C) over 16 - 24 hours and till a constant weight was achieved. Chemical testing was performed for all nutrients following the official methods of the Association of Official Analytical Chemists (AOAC).

2.2. Spectral measurements

The NIRS Analyzer measures the reflectance of leaves between 400-2500 nm, whereas the data generated by the WinISI software of the analyzer are displayed after converting to absorbance (log (1/reflectance)). The spectral observations of the leaves were taken within a black cup to reduce the impact of stray light (Figure 1.c). The leaves were trimmed symmetrically for all samples to fit the size of the cups. The spectral measurements were given at 0.5 nm interval with a total of 4,200 readings. The values of absorbance were converted back to reflectance values using the relationship of ($10^{-\text{Absorbance}}$). Rather than using the entire 4200 readings, one reading was taken in an interval of 8 nm, (i.e., every 16 readings because the spectral resolution is 0.5 nm) as a representative spectral signature, so that a total of 262 readings were used for data analysis. All subsequent steps were performed using the R statistical language (R Version 4.0.2; R Core Team, 2021).

2.3. Wavelength selection and development of models

In this research, a Pearson's correlation (*r*) analysis between the wavelengths range of 404 - 2492 nm and the content of each element was first performed. The absolute highest correlation values could potentially be considered as the key wavelengths for the statistical models. We used multiple linear regression (MLR) to build models of correlation between the chemical results of petioles and spectral results of leaves. The chemical results of petioles acted as responses (*y*) and the spectral results of the leaves within the range of 404 - 2492 nm functioned as predictors (*x*), resulting in the following model:

$$y = \beta_{\circ} + \sum_{i=1}^{Z_i} x_i \beta_i \tag{1}$$

In this dataset, the number of predictors is larger than the number of datapoints, which may result in over-fitting (Ye et al., 2020). Prediction accuracy thus can be improved by shrinking or setting some coefficients to zero using subset selection methods. Lasso MLR is one of the shrinkage methods that performs regularization and identifies the most informative, least redundant features to predict the responses (Hastie et al., 2008). Lasso is regulated by a complexity parameter λ, which controls the amount of shrinkage: the larger the value of λ is, the greater the penalization of the non-zero coefficients in the model can be, and consequently a greater shrinkage imposed on coefficient values can be achieved. Efficient algorithms are available for computing the entire path of solutions as λ is varied (Hastie et al., 2008). The model selects the value of λ which minimizes the root mean squared error (RMSE). The chosen λ parameter determines the number of coefficients that will compose the final model, which are selected as the ones with the greatest explanatory power in relation to the target variable.

Lasso was implemented using the *glmnet* and *caret* packages of the R statistical language (Friedman et al., 2010; Kuhn, 2022). Model training and performance assessment were conducted using 5-fold cross validation, with the value of λ chosen based on the smallest root mean squared error (RMSE). Table 3 shows the number of coefficients at the selected λ and the selected RMSE value by the model. Table 3 also shows the first four significant wavebands, as 4 bands are normally sufficient in NIRS analysis (Williams, 2019).

2.4. Model performance

The values of r^2 between the actual and estimated concentrations were calculated as the mean across the cross validation folds as shown in Table 4. The performance of the models was categorized based on the ratio of standard error of prediction (SEP) to standard deviation (SD) of actual concentrations (Williams, 2019), known as Ratio of (standard error of) Prediction to (standard) Deviation (RPD). This is calculated according to Equation (2).

$$\mathrm{RPD} = \frac{\sqrt{\langle\{\sum \mathrm{A}_\mathrm{n}^2 - [(\sum \mathrm{A}_\mathrm{n})^2 / C] / (C-1)\}\rangle}}{\sqrt{\langle\{\sum(\mathrm{A}_\mathrm{n}-\mathrm{E}_\mathrm{n})^2 - [\sum(\mathrm{A}_\mathrm{n}-\mathrm{E}_\mathrm{n})^2 / C]\}/(C-1)\rangle}} \quad (2)$$

The RPD for the prediction of functionality factors such as grain texture were categorized as excellent (> 4.1), very good (≥ 3.5 - 4.0), good (≥ 3.0 - 3.4), fair (≥2.5 – 2.9), and poor (< 2.0) as described by Williams (2019) who mentioned that SEP shall be considerably lower than the SD, and ideally the ratio of the SD to SEP should be 3 or higher. Another study for monitoring the foliar nutrients status of mango using spectral indices gave another classification for RPD as excellent (>2), acceptable (≥ 1.4 - 2.0) and nonreliable (< 1.40) (Mahajan et al., 2021). Considering that mango is a horticultural crop (Saúco, 1997) as potato crop (Agriculture and Agri Food Canada, 2020), we followed the latter classification.

3. Results and Discussion

3.1. Influence of temporal and spatial distribution on chemical analysis of potato petioles

The results obtained from the chemical analysis over the entire growing season are presented in Table 2, which shows the range of maximum and minimum results for each element with arithmetic mean values in comparison to the normal range of nutrients in potato petioles as recommended by A & L Canada Laboratories Inc in Ontario. The normal range is similar to what was recommended by the University of Minnesota for potato petioles (Kaiser and Rosen, 2018). The form of lab analysis commonly includes the chemical testing of macro nutrients in percentages (%) and micronutrients in particles per million (ppm) except for Na which is in percentage (%). Figure 2 shows the temporal concentration of each element and their distribution along with the normal range. Figure 2 also shows the spatial distribution of the measured concentrations whether their sampling was in the farm or indoor cultivation area. The common practice in New Brunswick is to add commercial fertilizers to soil such as NPK to reduce the potential for nutrient losses in latter stages. Ca and Mg are supplied through lime, while the micronutrients are only supplemented if a deficiency is observed (Government of New Brunswick, Department of Agriculture, Aquaculture and Fisheries, 1988). Based on those practices, the illustration in Figure 2 of the chemical content of nutrients are the common ranges of nutrients found in soil within the season. At this level of research, we did not perform any soil testing and we cannot ensure that the low concentrations of elements in petioles are due to deficiency in soil or stressed plants, as our focus is to find correlation between the nutrients' concentration in the petioles and the foliar spectral reflectance.

3.1.1. Dilution of NPK and S, and effects on micronutrients (Mn, Fe and Cu)

The high NPK concentrations in the beginning of the season refers to the current practice of largely applying fertilizers at early stages to fulfill the fertilizer requirements during plants' vegetative and reproductive stages and to avoid deficiencies later in the season (Figure 2.a, b, c). The decline of NPK during the growing season may be explained by the dilution phenomenon as plant biomass increases (Du et al., 2020; Gómez et al., 2020). The higher uptake of N, and P at late stages was also documented by Liu et al. (2021) and Rosen et al. (2014), respectively. While the slight increase in concentrations of the NPK at the end of the season may refer to the reason that potato plant uptake of NPK reached to the maturity phase of the tubers and NPK elements are no longer moving from foliage to underground tubers. Apparent trend was similarly noticed for S through the season and its uptake possibly refers to the translocation within the plant both for its contribution to plant yield and quality (Koch et al., 2020). Knowing that the application of S to potato plants is usually fertilized with K_2SO_4 instead of KCl, the elevation in S concentration would be referred to the high K application at the beginning of the season which was found in Figure 2.d in response to concentrations in Figure 2.c.

Another synergistic effect is potentially available between K, Mn, and Fe, as it was documented that the increasing level of K causes a larger uptake of Mn concentration (dos Anjos, and Monnerat, 2000), and excessive level of K might result in excessive uptake of Mn and Fe (Torabian et al., 2021). The link among K and Mn was noticed in our chemical results as shown in Figure 2.c, e till 80 days after planting. The random distribution of Mn concentration thereafter may raise doubts about the reliability of the chemical testing. On the other hand, the synergistic effect between K and Fe was found in our chemical results as shown in Figure 2.c, f, except three concentrations were found to be anomalous at one specific timing and this could refer to less reliability of chemical testing in that week of petiole analysis. On the other hand, Cu concentration was noticed to decrease with K's increase in the petioles as shown in Figure 2.c, g, and these results agree with a study done by dos Anjos, and Monnerat (2000).

3.1.2. Increasing uptake of Mg and Ca and their effects on micronutrients (Al, Zn and B)

Mg is recognized as a competitive cation to K for plant uptake (Koch et al., 2020). That means a low concentration of K in plant samples would cause a rise in Mg concentrations, which was the case towards the end of the season as shown in Figure 2.h. A previous study observed a similar phenomenon based on a cation antagonism between K and Mg, where there was a significant decrease in Mg concentrations with higher K supply in potato plants (Koch et al., 2019). In addition, the Ca concentrations have shown high values during the growing season (Fig 2.i) because of the probable transport of Ca via the xylem rather than being transported for tuber formation (Koch et al., 2020). Ca and Mg are commonly known for their contribution to maintain a stable pH in soil through the application of lime in the shape of $Ca.Mg(CO_3)_2$ (Government of New Brunswick, Department of Agriculture, Aquaculture and Fisheries, 2011).

The supply of Ca is commonly used not only to neutralise the soil pH but also to inhibit the uptake of Al and Mn that may cause toxicity to potato plants. This could explain the Al concentrations under the maximum normal range for both farm and indoor data as shown in Figure 2.j. Moreover, three concentrations of Al at one specific timing were higher than the normal range and this could refer to the non-reliability of chemical testing at this time of sampling.

Ca application will further impact the uptake of Zn due to the decrease in soil acidity. A previous study stated that when pH is raised by the addition of lime, Zn will be less available to potato plants (Koch et al., 2020) and this could justify the decrease in Zn concentrations after 70 days from planting (Figure 2.k) concurrently with the increase of Ca shown in Figure 2.i. Furthermore, low B concentrations was documented to be found in the acidic soils (Waqar et al., 2012). Therefore, the addition of lime in shape of Ca shall increase the B concentration uptake, which correspond to our chemical results shown in Figure 2.i, l.

3.2. Correlation analysis and Lasso MLR analysis

Table 3 shows the selected wavebands, most significant wavebands, and RMSE of the training model given by Lasso. These absorption bands of Vis-NIR are commonly known as overtones which can be assigned to specific functional groups. Sometimes two absorbers coincide to the extent that an absorption band appears near the sum of the frequencies of the two fundamental wavebands, and thus, we show the first four significant wavebands in Table 3 as recommended by Williams (2019). Figure 3 shows the results of the highest absolute r values between the petiole chemical contents and the reflectance of wavelength range from 404 - 2500 nm for both testing modes (dried and fresh leaves). The vertical bars of width 20 nm show the regions of the four most significant waveband given by the Lasso MLR models. This width is arbitrarily chosen to check whether the most significant wavebands would cross in the same range.

3.2.1. Pearson's correlation and Lasso MLR significant wavebands for macronutrients

Amongst all macronutrients, S gave the highest r value in the fresh testing mode as shown in Figure 3.a-f. A comparable result was given by Lasso MLR for S with close r^2 value in both modes (Table 4). Similarly, P and K were given highest r values in the dried testing mode (Figure 3.b, c), and Lasso MLR also gave indistinguishable r^2 values in both modes. In contrast to Pearson's correlation, Lasso MLR training model showed that N has highest r^2 values for the fresh testing mode as shown in Figure 3.a.

The most significant wavebands were in the Vis range for N, P and C as presented in Figure 3.a, b, d, except for one waveband found in the NIR range for K, Mg and S (Figure 3.c, e, f), which might possibly be related to the synergistic effect among them as explained earlier in Sections (3.1.1, 3.1.2). The significant wavebands in Vis range would probably explain having the highest correlation in fresh testing mode for N and K, in addition to P, and S as those wavebands will not interfere with water absorbance spectra in the NIR range (Prananto et al., 2020). Similar significant wavebands were concluded for P prediction in the VNIR region of the spectrum in corn canopy (Siedliska et al., 2021), and for S and K prediction at Vis- VNIR range of the spectrum in mango leaves (Mahajan et al., 2021).

3.2.2. Pearson's correlation and Lasso MLR significant wavebands for micronutrients excluding Na

All micronutrients show highest *r* values in the dried testing mode like the results given by Lasso MLR modelling, except for Fe that has a comparable r^2 value in both modes (Figure 3.g-m, Table 4). The four significant wavebands were found in Vis range only in Mn (Figure 3.g), while B had a solo significant waveband in NIR region (Figure 3.j) regardless its interference with Ca (Section 3.1.1), which possibly give a fingerprint for B. Amongst the elements, Zn, Fe, Cu, and Al had similarities in having two significant adjacent wavelengths in Vis and NIR (Figure 3.h,i,k,l), respectively, whilst those wavebands in the NIR range are not interfering with the significant waveband found for the macronutrient affecting them such as K and Ca (Sections 3.1.1, 3.1.2).

The above correlation analysis of the spectral data showed that the most significant wavebands were more prominent in the Vis-NIR region. These prominent spectral variations were also reported by Osco et al. (2020) for predicting macro and micronutrients in orange and by Ling et al. (2019) for detecting concentrations of leaf nutritional elements.

3.3. Estimation of concentrations and models performance

3.3.1. Lasso MLR models performance for macronutrients

The Lasso MLR results suggest excellent performance for estimating all macronutrients based on the RPD classification shown in Table 4 except for S that showed acceptable RPD value. Moreover, the high RPD values shown in Table 4 may provide supporting evidence that the generated models accounted for more of the variance in the datapoints represented by the chemical results shown in Figure 2.a-d, 2.h-i.

For instance, the vast majority of the N concentrations (93%) was above the normal range (2.49 - 3 %) (Figure 4.a), in spite of that, the model had reasonable estimation, likewise, for P estimation model presented in Figure 4.b. In addition, K, and Mg estimation models showed fair distribution around the fitting line despite being beyond the normal range (Figure 4.c, e). Mg estimation model gave a fairly distribution of estimated concentrations around the fitting line more than the concentrations above the normal range (Figure 4.e).

Only the Ca estimation showed a low correlation, but a high RPD value at 2.55 (Table 4), which would possibly refer to the fair variance in the actual measurements shown in Figure 2.i. S was the only macronutrient that had all concentrations below the normal range, nevertheless, its model performance gave reasonable results of r^2 and RPD values in comparison to other macronutrients (Table 4). For that reason, models of Ca and S may require enriching the datasets with more variability in chemical concentrations.

3.3.2. Lasso MLR models performance for micronutrients excluding Na

RPD evaluation hovered around acceptable to excellent performances for the estimation of all micronutrients as shown in Table 4. The Lasso MLR models unveiled considerably high correlation values except for Mn. Nevertheless, Mn estimation model showed an excellent RPD value (Table 4) which may correspond to the variance in the chemical concentrations shown in Figure 2.e. Al had less reliability in chemical concentrations at the beginning of season as explained in Section 1.3.2 and shown in Figure 2.j. Those unreliable concentrations of Al may have biased the model during training, especially since model selection was based on the lowest RMSE value. In Figure 4.l, the Al model shows good estimation results when the concentrations were under 300 ppm, and beyond 1000 ppm, three datapoints were shown to be underestimated. For that purpose, additional analysis was performed on Al dataset after re-grouping datapoints to avoid underfitting that occurred due to the high concentrations in the beginning of the season. After re-grouping, Lasso testing model showed an improvement in r^2 value from 0.67 to 0.71 and RPD value decreased slightly from 2.61 to 2.39. Moreover, when we considered the three datapoints shown at day 52 in Figure 2.j as out of accepted range of concentrations, the r^2 value of the testing model was marginally decreased from 0.67 to 0.62 and the RPD value increased from 2.61 to 3.78. Thus, further investigation is required for Al modelling, with larger datasets.

Likewise, Fe concentrations showed three inconsistent values in comparison to others within the growing season in Figure 2.f and Figure 4.i. Nevertheless, cross validation results of the Lasso model yielded r^2 value at 0.65 and RPD value at 3.66 (Table 4). This high value of RPD commonly means that a small error of estimation is found in comparison to actual values. However, we had less confidence of these three concentrations in comparison to the other Fe concentrations during the season. For that purpose, we re-assessed the model performance after dropping these three concentrations and the results showed a decrease in the r^2 value from 0.65 to 0.40 and RPD value from 4.23 to 4.24. Although r^2 was devalued, the range of the actual Fe concentrations entered for training the model are more reliable. For the other micronutrients, the concentrations were well estimated around the fitting line (Figure 4.g, h, j, k) and the model performance with regards to RPD gave an acceptable to excellent accuracy for Zn, Cu and Mn, B, respectively (Table 4).

3.4. Overall evaluation of the datasets and the developed models

The dataset was made of samples collected from 3 locations and had no more than 60 datapoints collected over one season. In our effort to maximize the range of observations in terms of different nutrient concentration, we took the samples over one season with an interval of two weeks between samples taken from the same subplot following the current protocol of sample collection, and preparation by potato growers in NB, Canada. This resulted in ranges that went higher, within and below the normal ranges for N, P, K, Mg, Zn and Mn (Figure 2.a, b, c, h, k, and l). We were able to extend the range of P in particular by the indoor cultivation area which used to apply P in concentrations that cannot be implemented in commercial farms. In the future, we will continue to use the indoor area to expand the ranges of other macronutrients as well as testing the models on wider ranges of observations.

This preliminary analysis assists in identifying the correlation between chemical contents of petioles and spectrum of leaves. Pearson's correlation was initially considered to find out whether any correlation would exist between the chemical contents of petioles and spectrum of leaves, and to highlight the wavebands that could potentially be considered as significant wavelengths. The testing mode of the highest Pearson's correlation agreed with the highest r^2 value given by Lasso MLR estimation models for all elements except N, S and Zn. The models showed that most significant wavebands were in the Vis-VNIR range for all macronutrients except Mg and S, which had significant third and fourth wavebands in SWIR. On the other hand, all micronutrients had the most significant wavebands in both Vis-VNIR and SWIR with a common significant waveband at 1932 nm, along with an adjacent waveband at 1940 nm. Similar results are supported by findings of other researchers such as N (Liu et al., 2020; Ye et al., 2020), P (Siedliska et al., 202), S and K (Mahajan et al., 2021). The visible correlation between the actual and estimated values of elements supported by reasonable RPD values shows a potential to estimate petiole elements based on foliar spectral reflectance in a lab-based level. The estimation models were trained by Lasso MLR on 48 datapoints and tested using the remaining datapoints, which we will enhance in the following seasons as we increase the number of datapoints used for the training and validation processes for all the models.

3.4.1. Correlation of Na

Na showed an exceptional pattern in comparison to other elements. The Na chemical content within the season showed a discrete distribution with a dominant concentration at 0.02% (Figure 2.m). These unchanging concentrations might be due to the reason that the chemical analysis of Na is based on the percentage unit rather than ppm, unlike the other micronutrients. The percentage unit might not be capable to describe changes in Na concentrations occurring within the season. Despite this discrete distribution in Na concentrations, the Pearson's correlation did not show an odd pattern in comparison to other elements as shown in Figure 3.m. In contrast, the Lasso MLR model gave a dominant estimation value at 0.02% (Figure 4.m) regardless to the other actual values up to 0.05 % shown in Figure 2.m. This estimation model resulted in a low r^2 value at 0.19 (Table 4). The RPD value at 4.36 (Table 4) indicates that the actual data variance is low, and thus the value for the RPD cannot be accurate to judge on the efficiency of the estimation capacity (Parrini et al., 2021). We are uncertain whether this low model performance happened as a reason for non-reliable chemical concentrations of Na or there is in fact no correlation between petiole Na content and leaf spectrum. Accordingly, we will remove Na from the analysis.

4. Conclusion

The results of this research show that there is a correlation between the chemical contents of potato petioles and leaf spectrum for all elements tested except Na. The models over the two testing modes show that most elements had higher correlation in the dried leaves except for N and K. Besides, the models showed potential to estimate P, S, and Fe in the fresh mode as stated in Table

4. These results set off a new technique to estimate petioles chemical contents based on two sets of foliar spectral reflectance: dried or fresh leaves.

5. Acknowledgment

This work is supported by; the Natural Sciences and Engineering Research Council of Canada (NSERC) under the Collaborative Research and Development Grant – Project (CRDPJ 543912-19), McCain Foods Limited, and Potatoes New Brunswick (PNB); and the New Brunswick Enabling Agricultural Research and Innovation (EARI) program of the Canadian Agricultural Partnership (CAP), project number: C1920-0056.

6. Declaration of Conflicting Interests

The authors declare no potential conflicts of interest with respect to the research, authorship, and/or publication of this article.

7. References

Agriculture and Agri-Food Canada (2020). Potato market information review – 2019-2020. https://www.agr.gc.ca/eng/canadas-agriculture-sectors/horticulture/horticulture-sector-reports/potato-market-information-review-2019-2020/?id=1606246042832 (accessed on May 31, 2021).

AL-Jobori, K.M.M., and AL-Hadithy, S.A. (2014). Response of potato (Solanum Tuberosum) to foliar application of iron, manganese, copper and zinc. International Journal of Agriculture and Crop Sciences (IJACS), 7 (7): 358-363. ISSN 2227-670X.Barczak, B., Nowak, K., and Knapowski, T. (2013). Potato yield is affected by sulphur form and rate. Agrochimica, 57 (4):363-372.

Bohl, W.H., and Johnson, S.B. (2010). Commercial potato production in North America: the potato association of America handbook, 2nd ed. Orono, United States.

https://potatoassociation.org/wp-content/uploads/2014/04/A_ProductionHandbook_Final_000.pdf (accessed on May 31, 2021).

Botha, E. J., Zebarth, B. J., and Leblon, B. (2006). Non-destructive estimation of potato leaf chlorophyll and protein contents from hyperspectral measurements using the PROSPECT radiative transfer model. Canadian Journal of Plant Science, 86 (1):279-91. https://doi.org/10.4141/P05-017.

Cohen, Y., Alchanatis, V., Zusman, Y., Dar, Z., Bonfil, D.J., Karnieli, A., Zilberman, A., Moulin, A., Ostrovsky, V., Levi, A., Brikman, R., and Shenker, M. (2010). Leaf nitrogen estimation in potato based on spectral data and on simulated bands of the VENμS satellite. Precision Agriculture, 11 (5): 520-37. https://doi.org/10.1007/s11119-009-9147-8.

Davenport, J.R., Perry, E.M., Lang, N.S., and Stevens, R.G. (2005). Leaf spectral reflectance for nondestructive measurement of plant nutrient status. HortTechnology, 15 (1):31-35. https://doi.org/10.21273/HORTTECH.15.1.0031.

dos Anjos, R. R. J. and Monnerat, P. H. (2000). Nutrient Concentrations in Potato Stem, Petiole and Leaflet in Response to Potassium Fertilizer. Scientia Agricola, 57 (2): 251–55. https://doi.org/10.1590/S0103-90162000000200009.

Du, L., Li, L., Li, L., Wu, Y., Zhou, F., Liu, B., Zhao, B. , Li, X., Liu, Q., Kong, F., and Yuan, J. (2020). Construction of a Critical Nitrogen Dilution Curve for Maize in Southwest China. Scientific Reports, 10 (1): 13084. https://doi.org/10.1038/s41598-020-70065-3.

Fageria, N. K., Barbosa Filho, M.P., Moreira, A., and Guimarães, C. M. (2009). Foliar fertilization of crop plants. Journl of Plant Nutrition, 32 (6): 1044-64. https://doi.org/10.1080/01904160902872826.

Friedman, J., Hastie, T., and Tibshirani, R. (2010). Regularization Paths for Generalized Linear Models via Coordinate Descent. Journal of Statistical Software, 33 (1): 1-22. https://www.jstatsoft.org/v33/i01/

Hastie, T., Tibshirani, R., and Friedman, J. (2008). The elements of statistical learning: data mining, inference, and prediction. Second edition. New York: Springer, 2008.

Herrmann, I., and Berger, K. (2021) Remote and proximal assessment of plant traits. Remote Sensing, 13:1893. https://doi.org/10.3390/ rs13101893.

Hochmuth, G. J., Maynard, D., Vavrina, C., Hanlon, E., and Simonne, E. (2018). Plant tissue analysis and interpretation for vegetable crops in Florida. Horticultural Sciences Department, UF/IFAS Extension, HS964 series. https://edis.ifas.ufl.edu/publication/ep081 (accessed on June 01, 2021).

International year of the potato (2008). North America. FAO. http://www.fao.org/potato-2008/en/world/northamerica.html (accessed on May 31, 2021).

Gabriel, J.L., Zarco-Tejada, P.J., López-Herrera, P. J., Pérez-Martín, E., Alonso-Ayuso, M., and Quemada, M. (2017). Airborne and ground level sensors for monitoring nitrogen status in a maize crop. Biosystems Engineering, 160:124-33. https://doi.org/10.1016/j.biosystemseng.2017.06.003.

Gómez, M.I., Magnitskiy, S., and Rodríguez, L.E. (2019). Critical Dilution Curves for Nitrogen, Phosphorus, and Potassium in Potato Group Andigenum. Agronomy Journal, 111 (1): 419–27. https://doi.org/10.2134/agronj2018.05.0357.

Kaiser, D.E., and Rosen, C.J. (2018). Understanding plant analysis for crops. University of Minnesota Extension. https://extension.umn.edu/testing-and-analysis/understanding-plant-analysis-crops (accessed on June 22, 2021).

Koch, M., Naumann, M., Pawelzik, E., Gransee, A., and Thiel, H. (2020). The importance of nutrient management for potato production part I: plant nutrition and yield. Potato Research, 63 (1):97-119. https://doi.org/10.1007/s11540-019-09431-2.

Koch, M., Busse, M., Naumann, M., Jákli, B., Smit, I., Cakmak, I., Hermans, C., and Pawelzik, E. (2019). Differential effects of varied potassium and magnesium nutrition on production and partitioning of photoassimilates in potato plants. Physiologia Plantarum, 166 (4):921-35. https://doi.org/10.1111/ppl.12846.

Kuhn, M. (2022). caret: Classification and Regression Training. R package version 6.0-91. https://CRAN.R-project.org/package=caret

Liao, H., Jianguo, W., Wenrong, C., Weidong, G., and Chunhai, S. (2012). Rapid diagnosis of nutrient elements in fingered citron leaf using near infrared reflectance spectroscopy. Journal of Plant Nutrition, 35 (11):1725- 34. https://doi.org/10.1080/01904167.2012.698352.

Ling, B., Goodin, D.G., Raynor, E.J., and Joern, A. (2019). Hyperspectral analysis of leaf pigments and nutritional elements in tallgrass prairie vegetation. Frontiers in Plant Science, 10: 142. https://doi.org/10.3389/fpls.2019.00142.

Liu, N., Townsend, P.A., Naber, M.R., Bethke, P.C., Hills, W.B., and Wang, Y. (2021). Hyperspectral imagery to monitor crop nutrient status within and across growing seasons. Remote Sensing of Environment, 255: 112303. https://doi.org/10.1016/j.rse.2021.112303.

Liu, N., Zhao, R., Qiao, L., Zhang, Y., Li, M., Sun, H., Xing, Z., and Wang, X. (2020). Growth stages classification of potato crop based on analysis of spectral response and variables optimization. Sensors, 20 (14): 3995. https://doi.org/10.3390/s20143995.

Mahajan, G. R., Das, B., Murgaokar, D., Herrmann, I., Berger, K., Sahoo, R.N., Patel, K., Desai, A., Morajkar, S., and Kulkarni, R.M. (2021). Monitoring the foliar nutrients status of mango using spectroscopy-based spectral indices and PLSR-combined machine learning models. Remote Sensing, 13 (4): 641. https://doi.org/10.3390/rs13040641.

Menesatti, P., Antonucci, F., Pallottino, F., Roccuzzo, G., Allegra, M., Stagno, F., and Intrigliolo, F. (2010). Estimation of Plant Nutritional Status by Vis–NIR Spectrophotometric Analysis on Orange Leaves [Citrus Sinensis (L) Osbeck Cv Tarocco]. Biosystems Engineering, 105 (4): 448–54. https://doi.org/10.1016/j.biosystemseng.2010.01.003.

Moinuddin, G., Jash, S., Sarkar, A., and Dasgupta, S. (2017). Response of potato (Solanum tuberosum L.) to foliar application of macro and micronutrients in the red and lateritic zone of west Bengal. Journal of Crop and Weed, 13 (1):185-188. ISSN: 0974-6315.

Motsara, M., and Roy, R.N. (2008) Guide to laboratory establishment for plant nutrient analysis. Food and agriculture organization of the United Nations, Rome.

Muñoz-Huerta, R.F., Guevara-Gonzalez, R.G., Contreras-Medina, L.M., Torres-Pacheco, I., Prado-Olivarez, J., and Ocampo-Velazquez, R. V. (2013). A review of methods for sensing the nitrogen status in plants: advantages, disadvantages and recent advances. Sensors, 13: 10823-10843. https://doi.org/10.3390/s130810823.

Naumann, M., Koch, M., Thiel, H., Gransee, A., and Pawelzik, E. (2020). The importance of nutrient management for potato production part II: plant nutrition and tuber quality. Potato Research, 63 (1): 121-37. https://doi.org/10.1007/s11540-019-09430-3.

Nigon, T.J., Yang, C., Paiao, G.D., Mulla, D.J., Knight, J.F., and Fernández, F.G. (2020). Prediction of Early Season Nitrogen Uptake in Maize Using High-Resolution Aerial Hyperspectral Imagery. Remote Sensing, 12 (8): 1234. https://doi.org/10.3390/rs12081234.

Osco, L.P., Ramos, A.P.M., Pinheiro, M.M.F., Moriya, É.A.S., Imai, N.N., Estrabis, N.V., Ianczyk, F., de Araújo, F.F., Liesenberg, V., de Castro Jorge, L.A., Li, J., Ma, L., Gonçalves, W.N., Marcato, J. J., and Creste, J. E. (2020). Machine learning framework to predict nutrient content in Valencia-Orange leaf hyperspectral measurements. Remote Sensing, 12 (6): 906. https://doi.org/10.3390/rs12060906.

Parrini, S., Staglianò, N., Bozzi, R., and Argenti, G. (2021). Can Grassland Chemical Quality Be Quantified Using Transform Near-Infrared Spectroscopy?. Animals, 12 (1): 86. https://doi.org/10.3390/ani12010086.

Peng, Y., Zhang, M., Xu, Z., Yang, T., Su, Y., Zhou, T., Wang, H., Wang, Y., and Lin, Y. (2020). Estimation of leaf nutrition status in degraded vegetation based on field survey and hyperspectral data. Scientific Reports, 10 (1): 4361. https://doi.org/10.1038/s41598-020-61294-7.

Povh, F.P., and dos Anjos, W.D.P.G. (2014). Optical sensors applied in agricultural crops. In Optical Sensors - New Developments and Practical Applications. edited by Yasin, M., Harun, S.W., Arof, H. (eds), InTech. ISBN: 978-953-51-1233-4. https://doi.org/10.5772/57145.

Prananto, A.J., Minasny, B., and Weaver, T. (2020). Near infrared (NIR) spectroscopy as a rapid and cost-effective method for nutrient analysis of plant leaf tissues. In Advances in Agronomy, 164:1-49. Elsevier. https://doi.org/10.1016/bs.agron.2020.06.001.

Rotbart, N, Schmilovitch, Z., Cohen, Y., Alchanatis, V., Erel, R., Ignat, T., Shenderey, C., Dag, A., and Yermiyahu, U. (2013). Estimating olive leaf nitrogen concentration using visible and near-infrared spectral reflectance. Biosystems Engineering, 114 (4):426-34. https://doi.org/10.1016/j.biosystemseng.2012.09.005.

Saari, H., Pellikka, I., Pesonen, L., Tuominen, S., Heikkilä, J., Holmlund, C., Mäkynen, J., Ojala, K., and Antila, T. (2011). Unmanned aerial vehicle (UAV) operated spectral camera system for forest and agriculture applications. Proceedings Volume 8174, Remote Sensing for

Agriculture, Ecosystems, and Hydrology XIII; 81740H. Event: SPIE Remote Sensing, Prague, Czech Republic. https://doi.org/10.1117/12.897585.

Saúco, V. (1997). Horticultural practices of mango. Acta Horticulturae, 455:391-400 https://doi.org/10.17660/ActaHortic.1997.455.50.

R Core Team (2021). R: A language and environment for statistical computing. R Foundation for Statistical Computing, Vienna, Austria. https://www.R-project.org/.

Rosen, C.J., Kelling, K.A., Stark, J.C., and Porter, G.A. (2014). Optimizing phosphorus fertilizer management in potato production. American Journal of Potato Research, 91:145-160. https://doi.org/10.1007/s12230-014-9371-2.

Rowe, R.C. (1993). Potato Health Management: The American Phytopathological Society. APS Press, Minnesota: 1-178.

Sharifi, M., Cheema, M., McVicar, K., LeBlanc, L., and Fillmore, S. (2013). Evaluation of liming properties and potassium bioavailability of three Atlantic Canada wood ash sources. Canadian Journal of Plant Science, 93 (6):1209-16. https://doi.org/10.4141/cjps2013-168.

Siedliska, A., Baranowski, P., Pastuszka-Woźniak, J., Zubik, M., and Krzyszczak, J. (2021). Identification of plant leaf phosphorus content at different growth stages based on hyperspectral reflectance. BMC Plant Biology, 21 (1):28. https://doi.org/10.1186/s12870-020-02807-4.

Government of New Brunswick, Department of Agriculture, Aquaculture and Fisheries (2011). Crop fertilization guide. The Land Development Branch. https://www2.gnb.ca/content/dam/gnb/Departments/10/pdf/Agriculture/Fertilityguide2001.pdf (accessed on August 05, 2021).

Government of New Brunswick, and the Department of Agriculture, Aquaculture and Fisheries (1988). Fertilizer. Agdex No. 200.21.

https://www2.gnb.ca/content/gnb/en/departments/10/agriculture/content/crops/nursery_landscape/fertilizer.html (accessed on February 09, 2022).

Torabian, S., Farhangi-Abriz, S., Qin, R., Noulas, C., Sathuvalli, V., Charlton, B., and Loka, D.A. (2021). Potassium: a vital macronutrient in potato production- a review. Agronomy, 11 (3): 543. https://doi.org/10.3390/agronomy11030543.

Waqar, A., Zia, M.H., Malhi, S.S., Niaz, A., and Saifullah (2012). Boron Deficiency in Soils and Crops: A Review, Crop Plant, Dr Aakash Goyal (Ed.), InTech. ISBN: 978-953-51-0527-5. http://www.intechopen.com/books/crop-plant/boron-deficiency-in-soils-and-crops-a-review

Williams, P., Antoniszyn, J., and Manley, M. (2019). Near infrared technology: getting the best out of Light. AFRICAN SUN MeDIA. http://doi.org/10.18820/9781928480310.

Xue, J., and Su, B. (2017). Significant Remote Sensing Vegetation Indices: A Review of Developments and Applications. Journal of Sensors: 1–17. https://doi.org/10.1155/2017/1353691.

Ye, X., Abe, S., and Zhang, S. (2020). Estimation and mapping of nitrogen content in apple trees at leaf and canopy levels using hyperspectral imaging. Precision Agriculture, 21: 198-225. https://doi.org/10.1007/s11119-019-09661-x.

Zebarth, B., Moreau, G., and Karemangingo, C. (2007). Nitrogen management for potatoes: petiole nitrate testing. GHG Taking Charge Team Factsheet. https://www.soilcc.ca/ggmp_fact_sheets/pdf/Potato_pnit.pdf (accessed on June 17, 2021).

Zebarth, B. J., Leclerc, Y., Moreau, G., and Botha, E. (2004). Rate and timing of nitrogen fertilization of Russet Burbank potato: Yield and processing quality. Canadian journal of plant science, 84 (3): 855-863. https://doi.org/10.4141/P03-123.

Zerner, M., and Parker, K. (2019). Rapid assessment of crop nitrogen and stress status - in-field assessment of a hand-held near infrared tool. https://grdc.com.au/resources-and-publications/grdc-update-papers/tab-content/grdc-update-papers/2019/02/rapid-assessment-of-crop-nitrogen-and-stress-statusin-field-assessment-of-a-hand-held-near-infrared-tool (accessed on July 04, 2021).

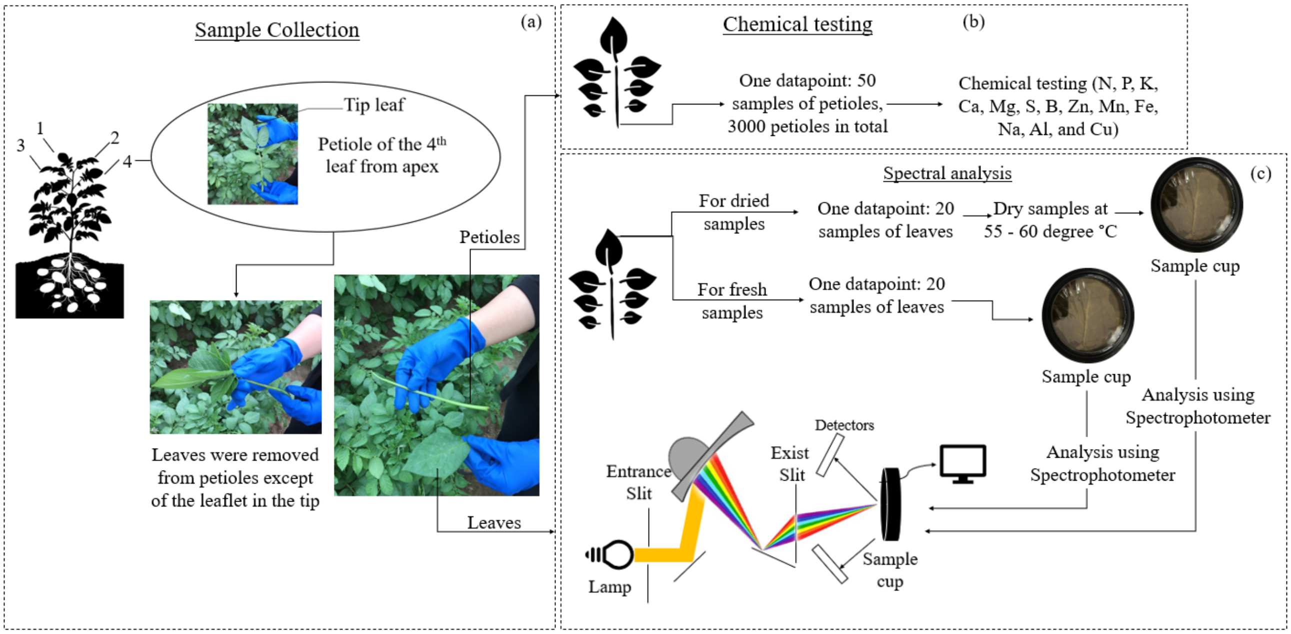

Figure 1. (a) Steps of sample collection. (b) Chemical testing. (c) Spectral analysis performed over the two modes of dried and fresh leaves.

Figure 2 Click here to access/download;Figure;Figure 2.docx

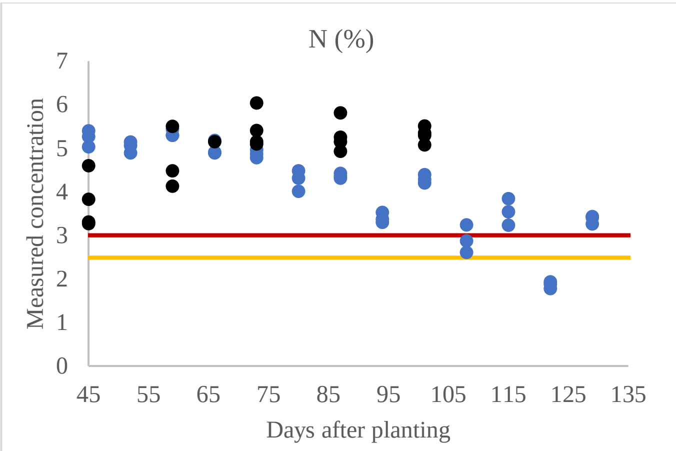

(a)

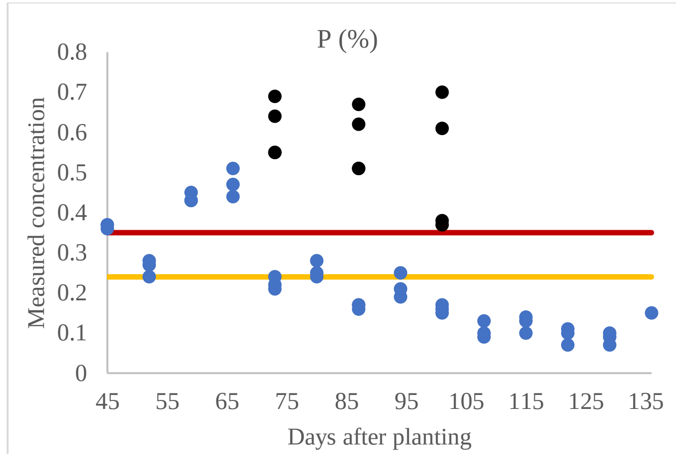

(b)

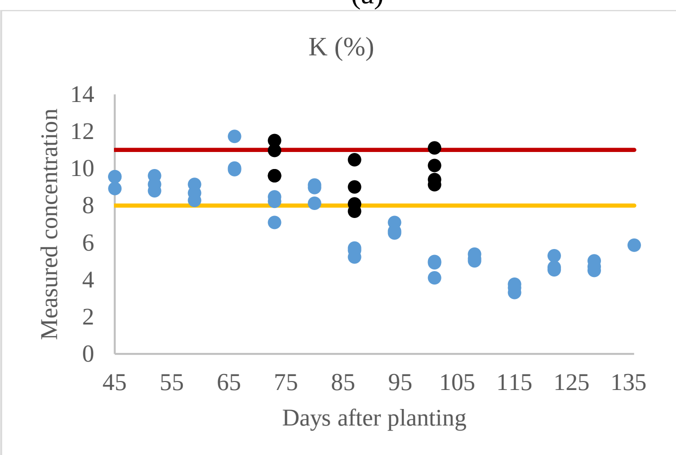

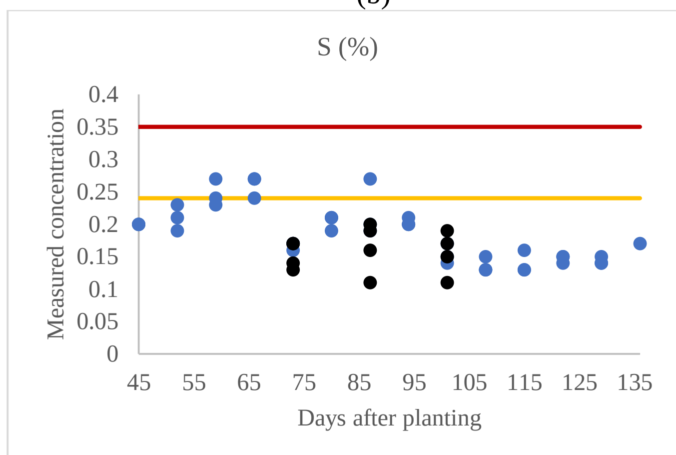

(c)

(d)

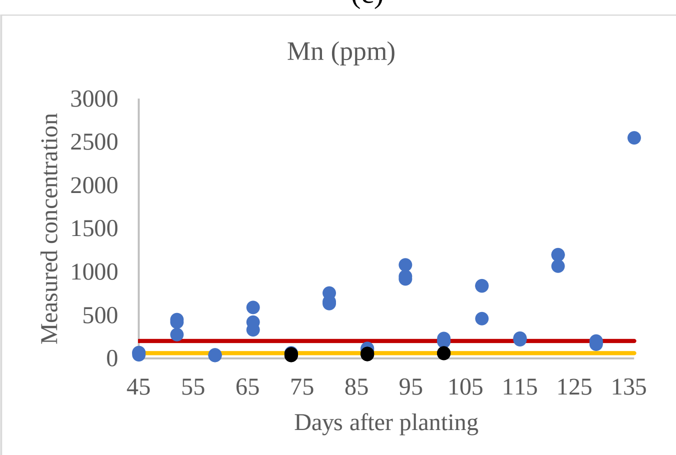

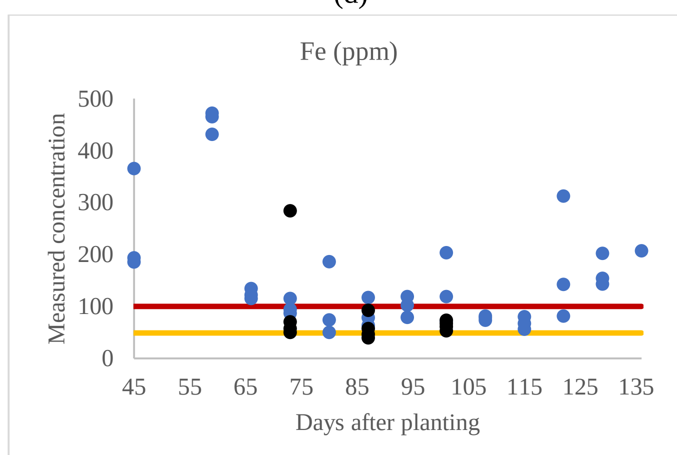

(e)

(f)

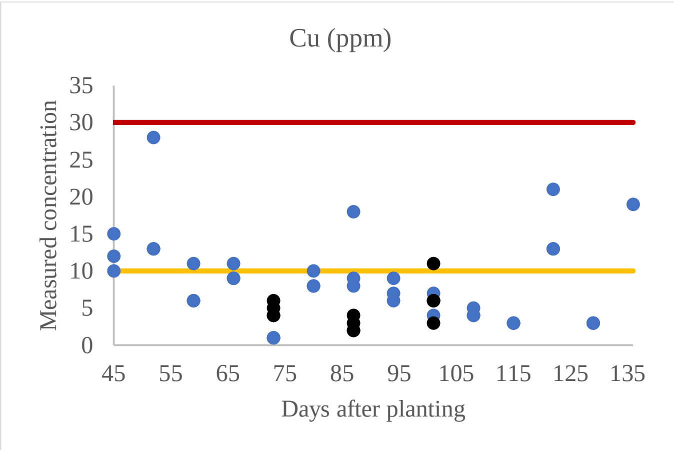

Cu (ppm)
Measured concentration
0
5
10
15
20
25
30
35
45
55
65
75
85
95
105
115
125
135
Days after planting

(g)

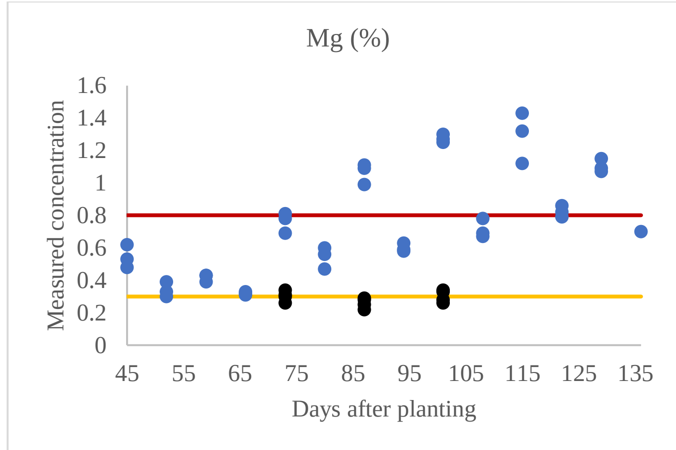

Mg (%)
Measured concentration
0
0.2
0.4
0.6
0.8
1
1.2
1.4
1.6
45
55
65
75
85
95
105
115
125
135
Days after planting

(h)

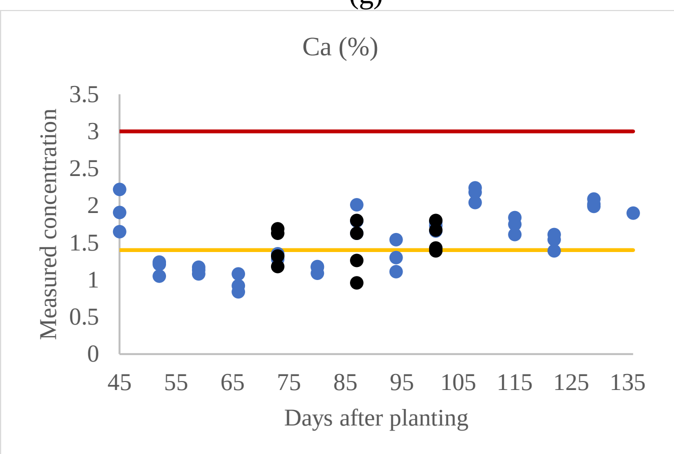

Ca (%)
Measured concentration
0
0.5
1
1.5
2
2.5
3
3.5
45
55
65
75
85
95
105
115
125
135
Days after planting

(i)

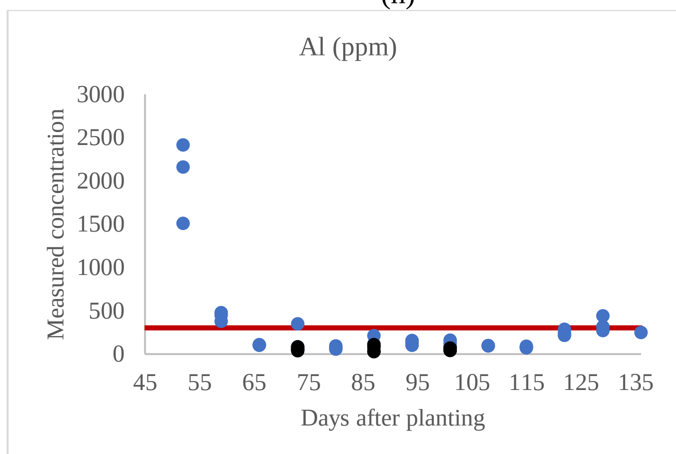

Al (ppm)
Measured concentration
0
500
1000
1500
2000
2500
3000
45
55
65
75
85
95
105
115
125
135
Days after planting

(j)

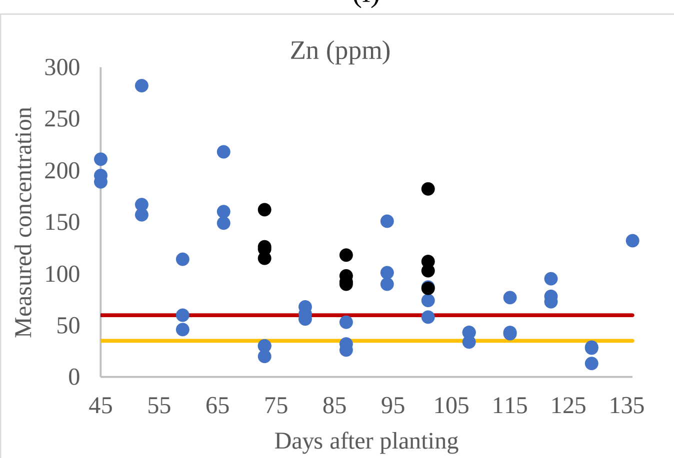

Zn (ppm)
Measured concentration
0
50
100
150
200
250
300
45
55
65
75
85
95
105
115
125
135
Days after planting

(k)

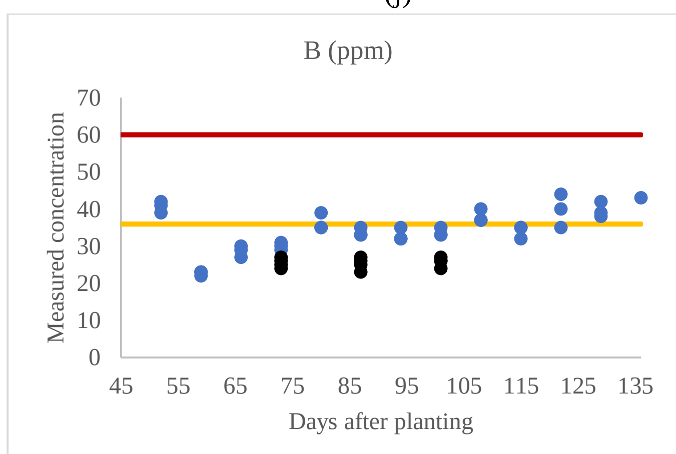

B (ppm)
Measured concentration
0
10
20
30
40
50
60
70
45
55
65
75
85
95
105
115
125
135
Days after planting

(l)

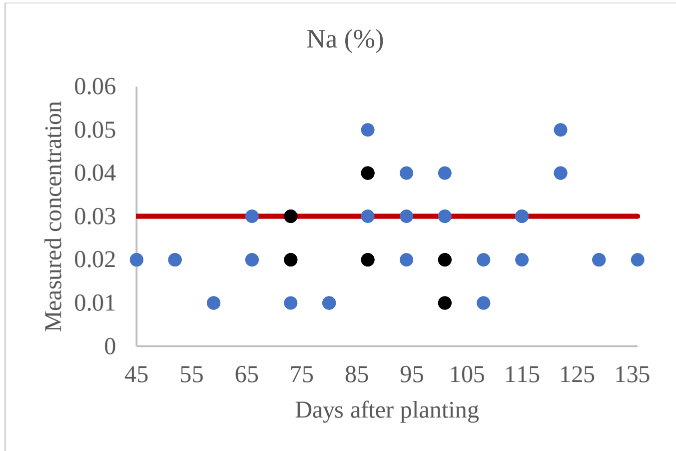

(m)

Figure 2. Temporal distribution for each nutrient during the growing season. Horizontal lines represent the limits of the maximum ( ) and minimum ( ) range of nutrients in potato petioles as recommended by A & L Canada Laboratories Inc in Ontario. , presents farm and indoor data, respectively.

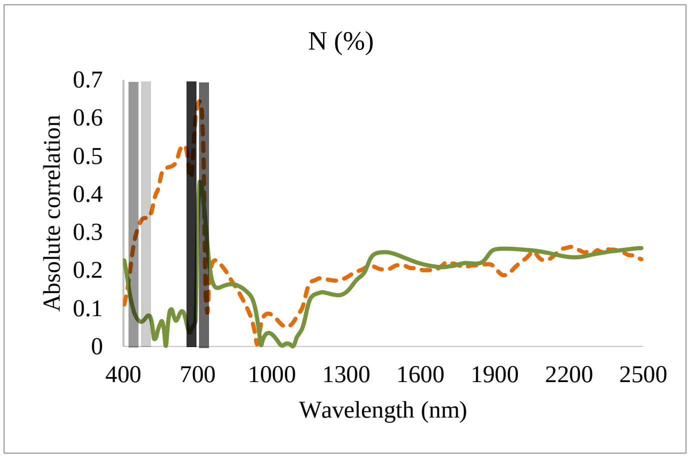
N (%)
Absolute correlation
0.7
0.6
0.5
0.4
0.3
0.2
0.1
0
400 700 1000 1300 1600 1900 2200 2500
Wavelength (nm)

(a)

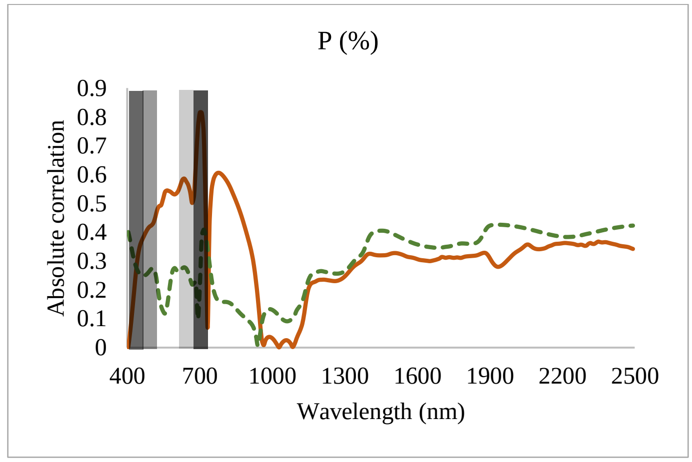
P (%)
Absolute correlation
0.9
0.8
0.7
0.6
0.5
0.4
0.3
0.2
0.1
0
400 700 1000 1300 1600 1900 2200 2500
Wavelength (nm)

(b)

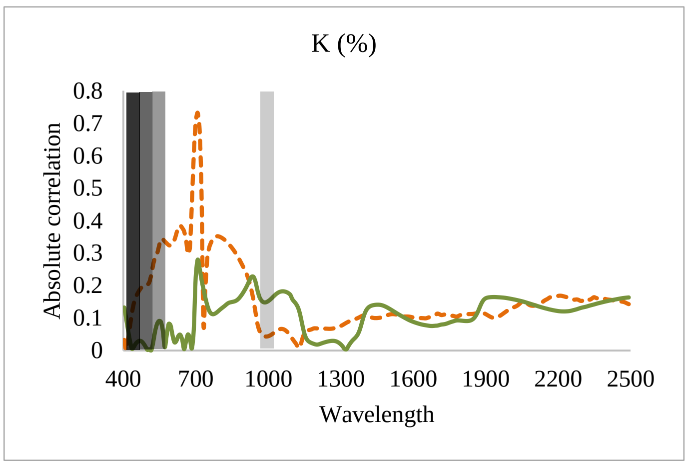
K (%)
Absolute correlation
0.8
0.7
0.6
0.5
0.4
0.3
0.2
0.1
0
400 700 1000 1300 1600 1900 2200 2500
Wavelength

(c)

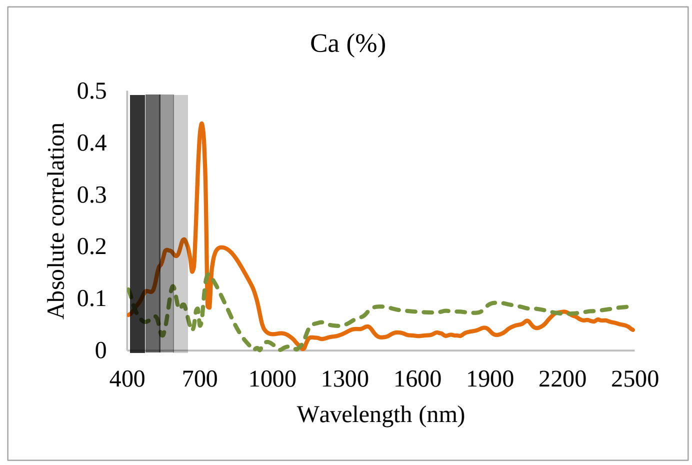
Ca (%)
Absolute correlation
0.5
0.4
0.3
0.2
0.1
0
400 700 1000 1300 1600 1900 2200 2500
Wavelength (nm)

(d)

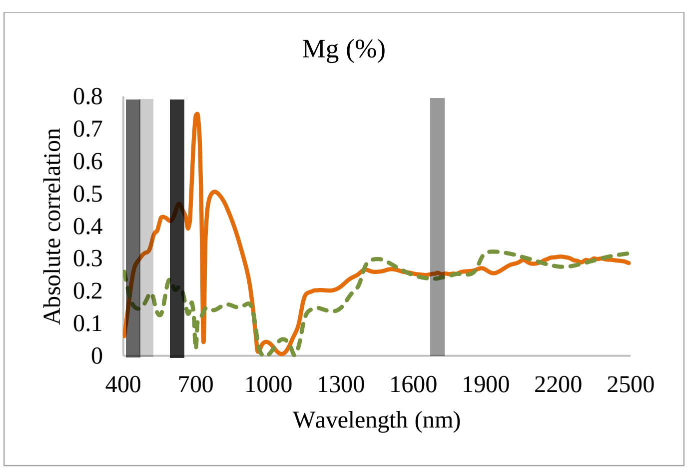
Mg (%)
Absolute correlation
0.8
0.7
0.6
0.5
0.4
0.3
0.2
0.1
0
400 700 1000 1300 1600 1900 2200 2500
Wavelength (nm)

(e)

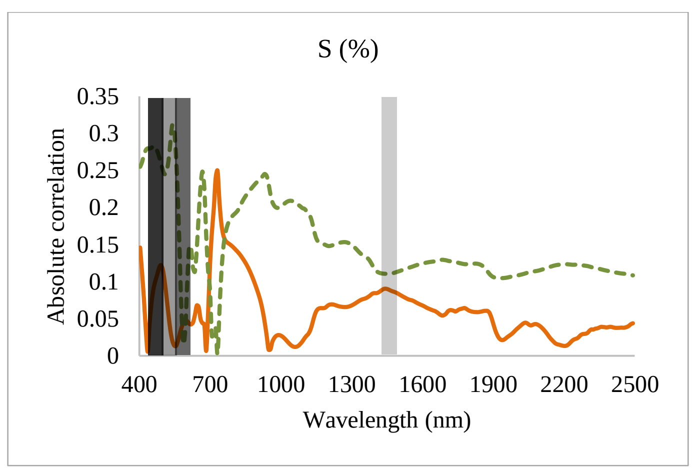
S (%)
Absolute correlation
0.35
0.3
0.25
0.2
0.15
0.1
0.05
0
400 700 1000 1300 1600 1900 2200 2500
Wavelength (nm)

(f)

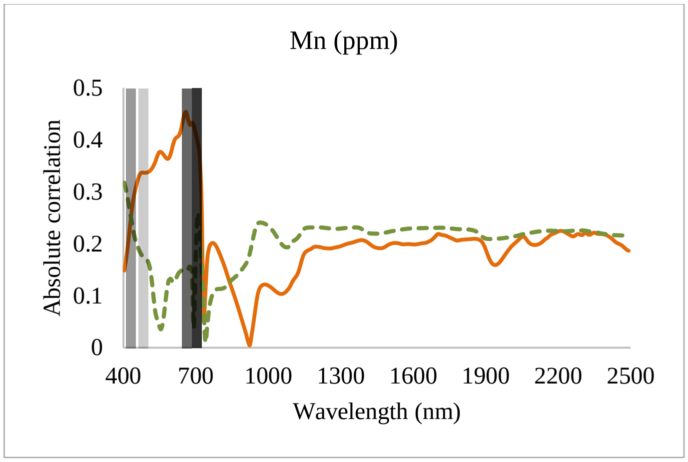
Mn (ppm)
0.5
0.4
0.3
0.2
0.1
0
Absolute correlation
400 700 1000 1300 1600 1900 2200 2500
Wavelength (nm)

(g)

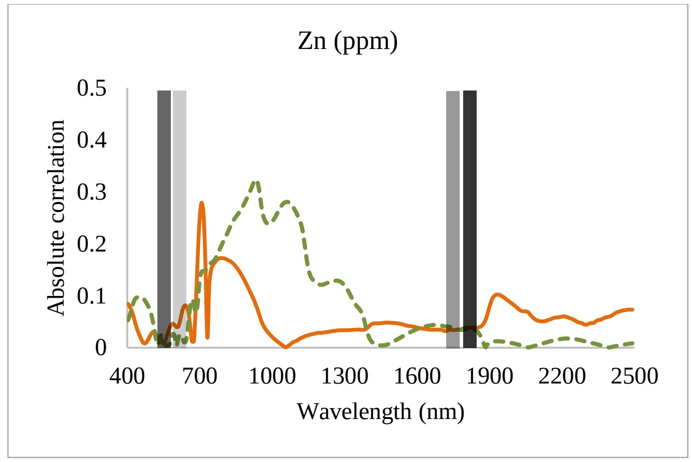
Zn (ppm)
0.5
0.4
0.3
0.2
0.1
0
Absolute correlation
400 700 1000 1300 1600 1900 2200 2500
Wavelength (nm)

(h)

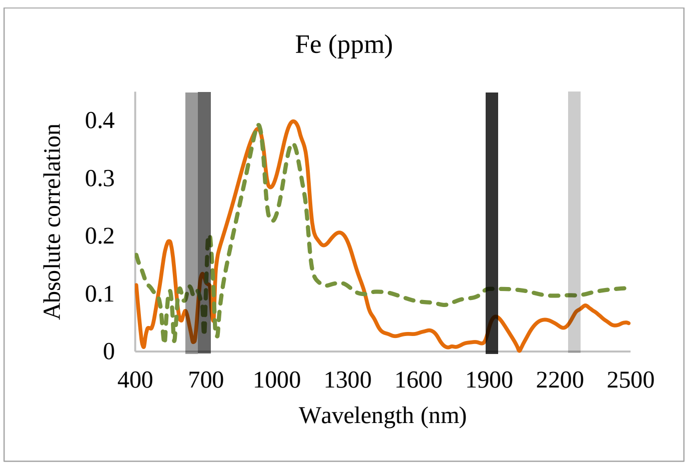
Fe (ppm)
0.4
0.3
0.2
0.1
0
Absolute correlation
400 700 1000 1300 1600 1900 2200 2500
Wavelength (nm)

(i)

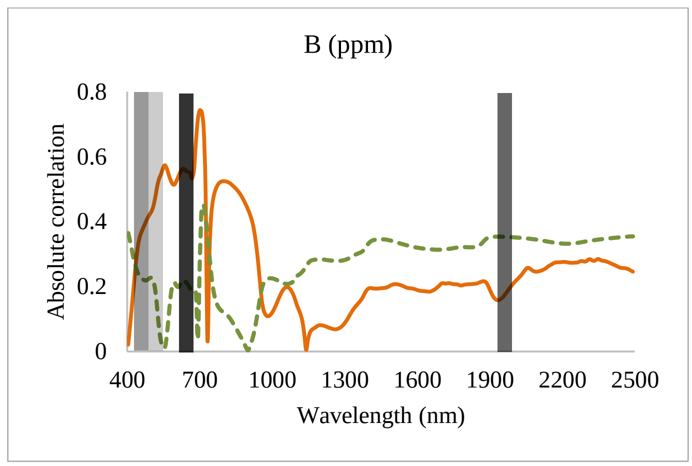
B (ppm)
0.8
0.6
0.4
0.2
0
Absolute correlation
400 700 1000 1300 1600 1900 2200 2500
Wavelength (nm)

(j)

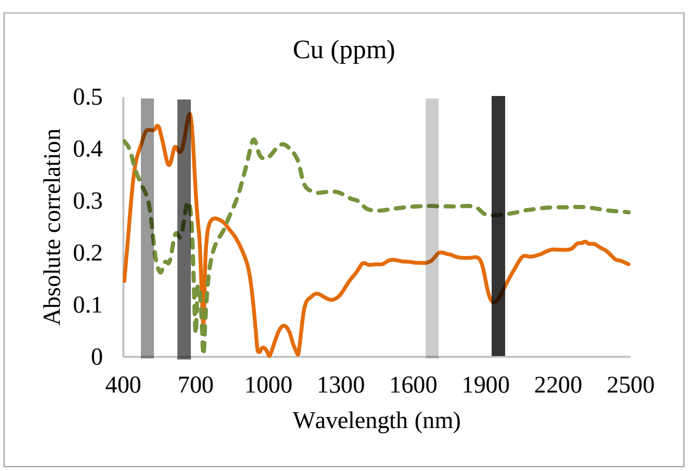
Cu (ppm)
0.5
0.4
0.3
0.2
0.1
0
Absolute correlation
400 700 1000 1300 1600 1900 2200 2500
Wavelength (nm)

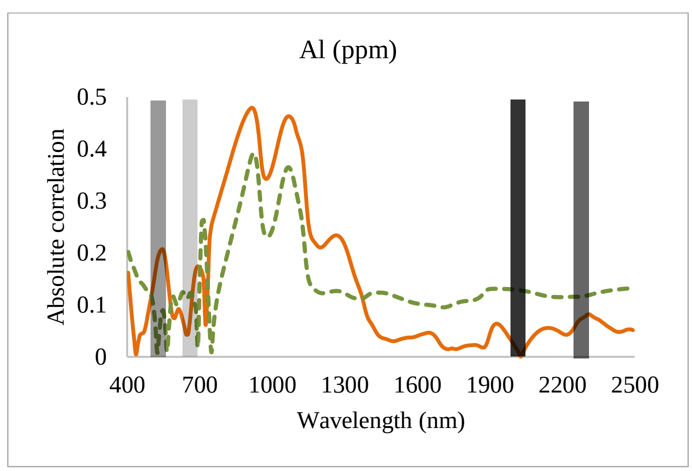
Al (ppm)
0.5
0.4
0.3
0.2
0.1
0
Absolute correlation
400 700 1000 1300 1600 1900 2200 2500
Wavelength (nm)

(k) (l)

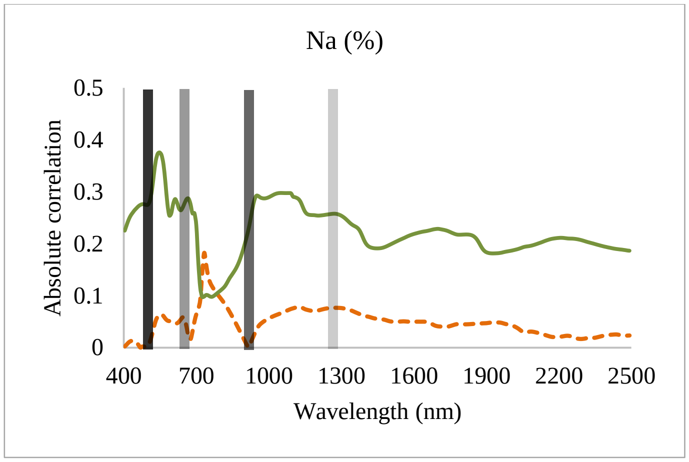

(m)

Figure 3. Pearson's correlation (*r*) for dried (—) and fresh leaves (—) across the spectrum. Absolute peaks represent the highest *r*. The solid line outlines the testing mode of the highest coefficient of determination (r^2) using Lasso Regression, while dashed line represents the testing mode with less r^2. The bars present the region of the four most significant wavebands by Lasso Regression. The intensity of the grey scale of the bars intensity gives the sequence of important wavebands from darker to brighter.

Figure 4

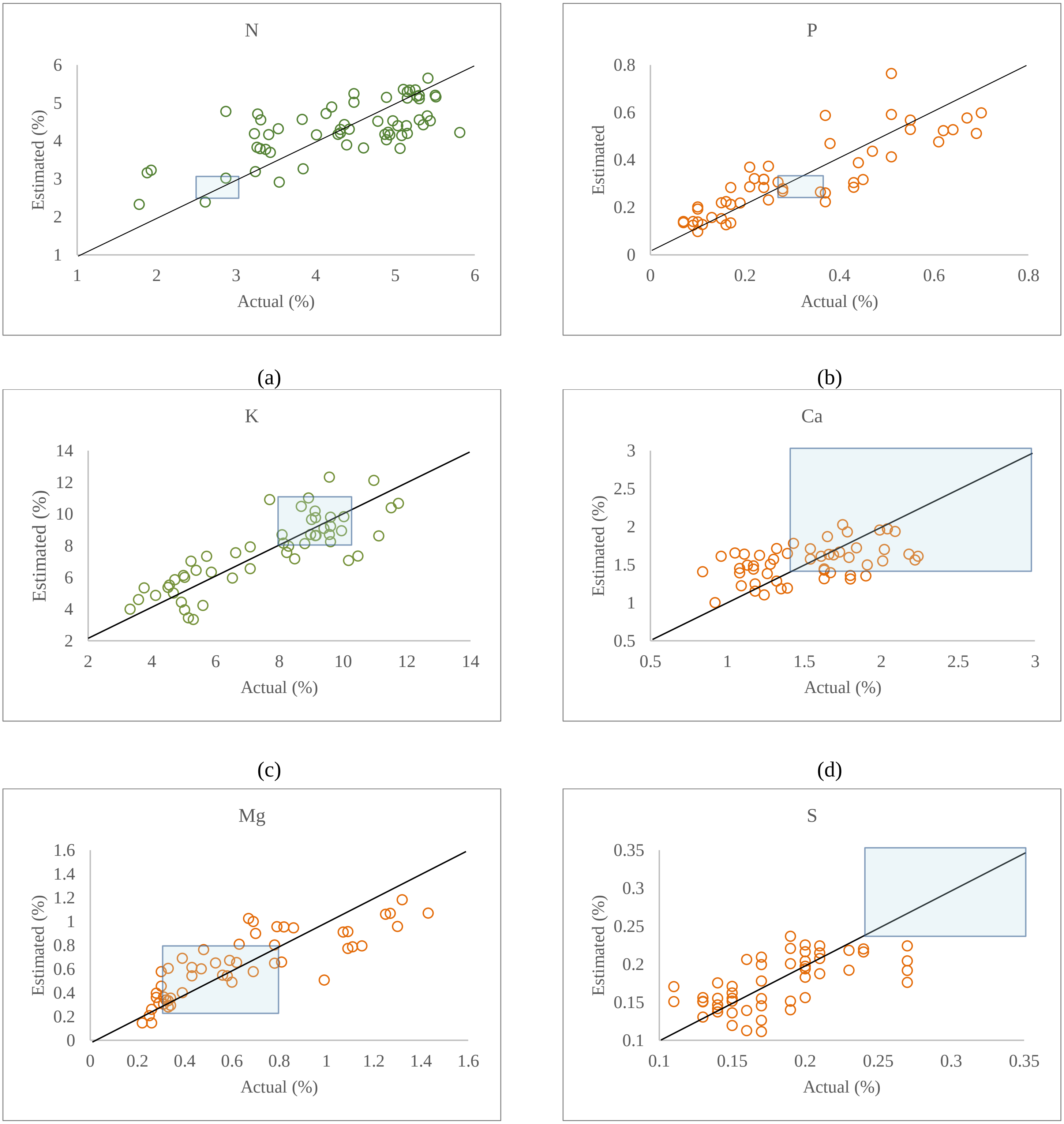

(a) (b) (c) (d) (e) (f)

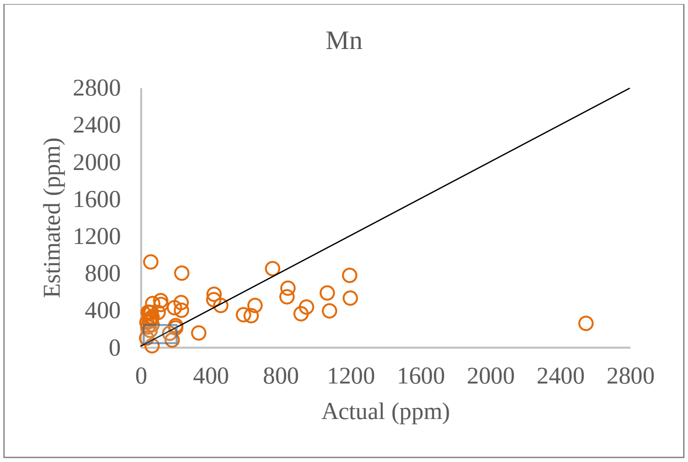
Mn
Estimated (ppm)
2800
2400
2000
1600
1200
800
400
0
0 400 800 1200 1600 2000 2400 2800
Actual (ppm)

(g)

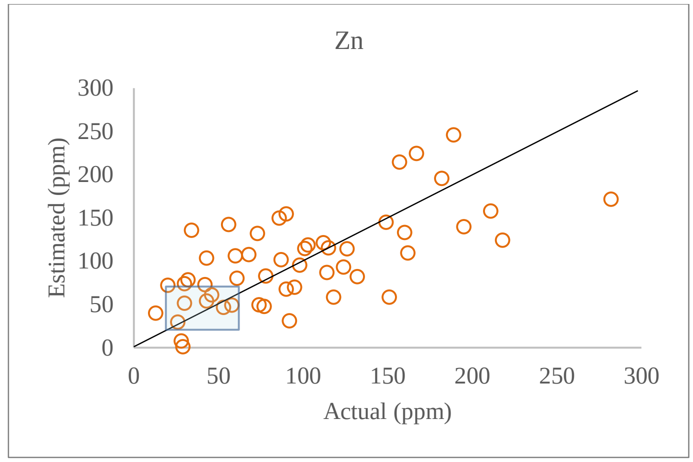
Zn
Estimated (ppm)
300
250
200
150
100
50
0
0 50 100 150 200 250 300
Actual (ppm)

(h)

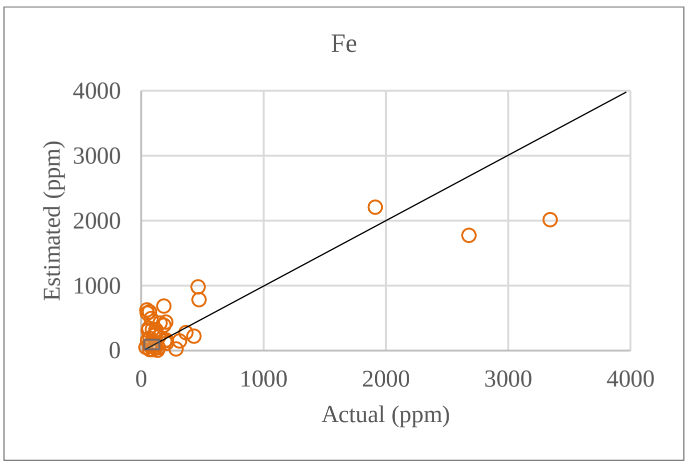
Fe
Estimated (ppm)
4000
3000
2000
1000
0
0 1000 2000 3000 4000
Actual (ppm)

(i)

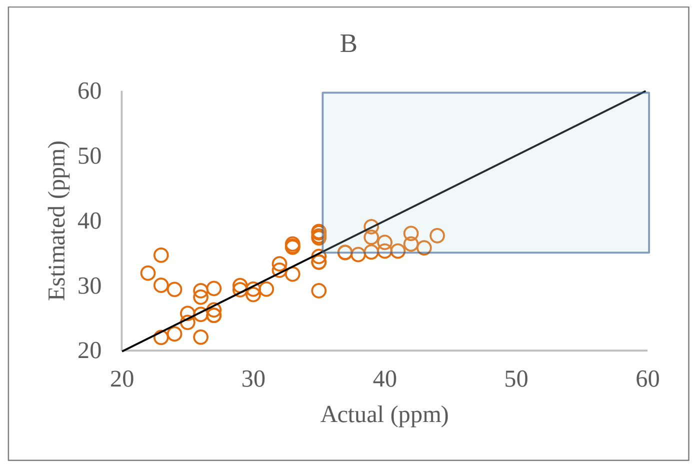
B
Estimated (ppm)
60
50
40
30
20
20 30 40 50 60
Actual (ppm)

(j)

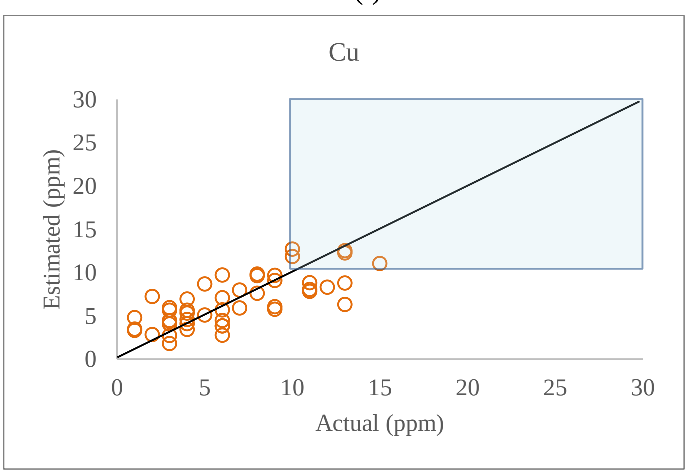
Cu
Estimated (ppm)
30
25
20
15
10
5
0
0 5 10 15 20 25 30
Actual (ppm)

(k)

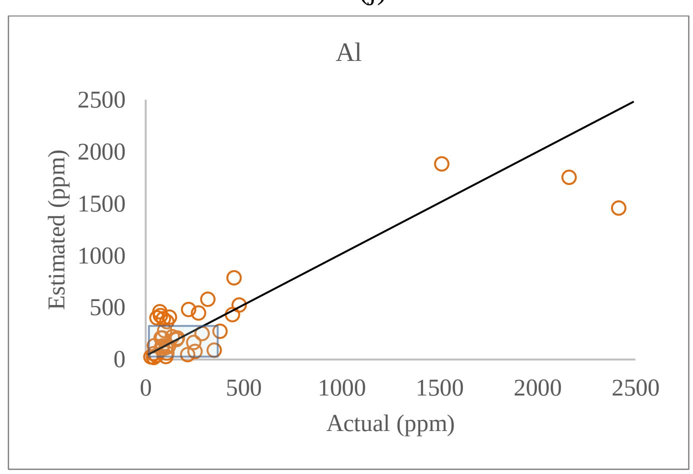
Al
Estimated (ppm)
2500
2000
1500
1000
500
0
0 500 1000 1500 2000 2500
Actual (ppm)

(l)

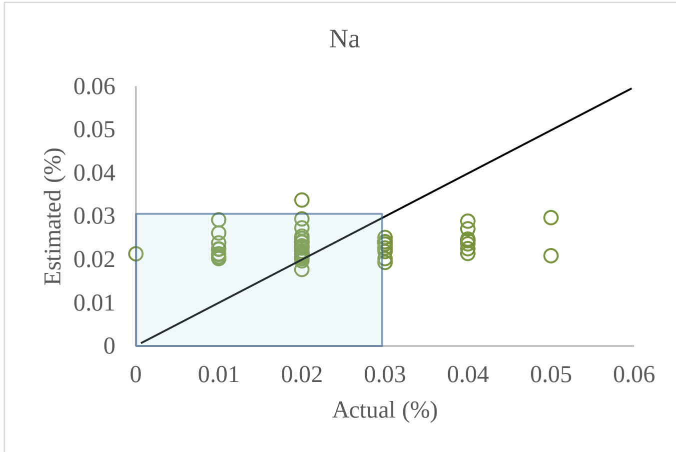

(m)

Figure 4. Validation results of the actual versus estimated concentrations of the testing mode (green for fresh, brown for dried) of the highest coefficient of determination (r^2). shows the normal range of nutrients in potato petioles as recommended by A & L Canada Laboratories.

Table 1. Operating specifications of NIRS DS2500 Analyzer

Item	**Specification**
Measurement Mode	Reflectance
Wavelength Range	400 - 2500 nm
Detectors	Silicon (400 - 1100 nm) and Lead Sulfide (1100 - 2500 nm)
Optical Bandwidth	8.75 ±0.1 nm
Spectral resolution	0.5 nm
Number of data points	4200
Wavelength Accuracy	± 0.05 nm

Table 2. Descriptive content of petiole nutritional concentrations during the entire growth season

Parameter	N (%)	P (%)	K (%)	Ca (%)	Mg (%)	S (%)	Mn (ppm)	Zn (ppm)	Fe (ppm)	Na (%)	Cu (ppm)	Al (ppm)	B (ppm)
Number of datapoints	60	52	52	52	52	52	52	52	52	50	52	49	49
Maximum measured	6.04	0.70	11.74	2.24	1.43	0.27	2545	282	3343	0.05	28	2415	44
Maximum recommended*	2.49	0.35	11	3	0.8	0.35	200	60	100	0.03	30	300	60
Minimum measured	1.78	0.07	3.32	0.84	0.22	0.11	31	13	49	0.01	1	26	22
Minimum recommended*	3	0.24	8	1.4	0.3	0.24	60	35	50	ND	10	ND	36
Mean	4.36	0.31	7.54	1.53	0.64	0.18	360	96	280	0.02	8	263	32
SD	1.02	0.19	2.36	0.37	0.35	0.04	471.36	59.97	621.98	0.01	5.52	483.99	6.16

* Normal range in nutrient concentrations stated by A & L Canada Laboratories Inc. ND: not defined

Table 3. Number, range, and first four significant wavebands resulting from Lasso MLR modelling at the better testing mode of each element

Element	Better testing mode	Number of bands	Range of bands (nm)	First four significant wavebands (nm)	RMSE value
N	Fresh	13	404 - 1828	660, 684, 404, 484	0.64
P	Dried	10	404 - 1924	708, 404, 540, 700	0.10
K	Fresh	17	404 - 2300	404, 428, 588, 948	1.23
Ca	Dried	20	404 - 2100	404, 444, 588, 540	0.30
Mg	Dried	14	404 - 1940	700, 532, 1716, 524	0.18
S	Dried	18	404 - 1916	404, 588, 516, 1452	0.03
Mn	Dried	22	428 - 2492	660, 628, 428, 492	377.41
Zn	Dried	12	468 - 2124	1932, 524, 1852, 532	49.11
Fe	Dried	19	404 - 2316	1932, 636, 524, 2308	329.70
B	Dried	11	412 -1932	684, 1932, 412, 460	232.62
Cu	Dried	23	428 - 2484	1940, 676, 428, 1716	2.48
Al	Dried	17	404 - 2316	1932, 2308, 524, 652	232.62
Na	Fresh	20	548 - 2148	548, 972, 700, 1028	0.01

Table 4. Validation results of Lasso MLR models estimating elements.

Element	Unit	Testing mode used for modelling	Validation results	
			r^2	RPD
N	%	Fresh	0.59	3.06
P	%	Dried	0.74*	2.26
K	%	Fresh	0.75**	2.44
Ca	%	Dried	0.32	2.55
Mg	%	Dried	0.77	2.85
S	%	Dried	0.50*	1.82
Mn	ppm	Dried	0.24	2.30
Zn	ppm	Dried	0.54	2.26
Fe	ppm	Dried	0.65*	3.66
B	ppm	Dried	0.62	2.08
Cu	ppm	Dried	0.58	2.09
Al	ppm	Dried	0.67	2.61
Na	%	Fresh	0.19	4.36

* r^2 values are < 0.04 compared to values of the fresh mode

** r^2 values are < 0.02 compared to values of the dried mode